



Heriot-Watt University

Heriot-Watt University
Research Gateway

Terrestrial Laser Scanning and Continuous Wavelet Transform for Controlling Surface Flatness in Construction - A First Investigation

Bosche, Frederic Nicolas; Biotteau, Baptiste

Published in:
Advanced Engineering Informatics

Publication date:
2015

[Link to publication in Heriot-Watt Research Gateway](#)

Citation for published version (APA):
Bosché, F., & Biotteau, B. (2015). Terrestrial Laser Scanning and Continuous Wavelet Transform for Controlling Surface Flatness in Construction - A First Investigation. Advanced Engineering Informatics.



Terrestrial Laser Scanning and Continuous Wavelet Transform for Controlling Surface Flatness in Construction – A First Investigation

Frédéric Bosché*, Baptiste Biotteau**

*School of Energy, Geoscience, Infrastructure and Society,
Heriot-Watt University,
EH14 4AS, Edinburgh, UK*

Abstract

We propose a novel approach to surface flatness characterization in construction that relies on the combination of Terrestrial Laser Scanning (TLS) and the Continuous Wavelet Transform (CWT). The former has the advantage over existing measurement technologies of providing both accurate and extremely dense measurement over surfaces. The latter provides the means to conduct frequency analysis with high resolution in both the space and frequency domains. This novel approach is tested using two real concrete floors and the results compared with those obtained with the Waviness Index method. The results show a high level of correlation. In fact, the proposed approach delivers a higher level of precision in the frequency and spatial domains. We also show what seems to be a weakness of the Waviness Index method in the detection of undulation with short periods. Finally, although not experimentally demonstrated here, the proposed method has the very interesting additional advantage of being applicable in 2D, that is over an entire surface instead of sampled survey lines (1D).

Keywords: laser scanning, quality control, tolerance, flatness, Wavelet Transform

*Corresponding author

**Visiting Scholar from Polytech-Nantes, Université de Nantes
Email address: f.n.bosche@hw.ac.uk (Frédéric Bosché)

1. Introduction

In construction, errors in the geometry of built components can have detrimental effects on the subsequent construction stages and/or the operation of completed facilities [1]. As a result, geometric tolerance control must be frequently conducted during construction projects.

1.1. Surface flatness control

Surface *flatness*, or surface *regularity*, is “the deviation in height of the surface [...] over short distances in a local area” [2]. The level of flatness may be specified for surfaces that are horizontal, vertical or sloped, and/or that are made of different materials. But, surface flatness is most commonly considered for concrete slabs/floors or screeds. Three main methods are generally considered for the control of surface regularity: the Straightedge method, the F-Numbers method, and the Waviness Index method. They are reviewed in the following paragraphs.

Straightedge method [2, 3, 4, 5]. This is the oldest and least accurate method, but it is still commonly used due to its ease of application. In the Straightedge method, the surveyor lays a straightedge at different locations on the surface and measures the maximum deviation under it, preferably using a stainless steel slip gauge [2]. The deviation is then compared to a specified tolerance to validate or reject the level of flatness of the surface (*e.g.* see specifications BS EN 13670 [3], BS 8204 [2] and [4] in the UK; ACI 117 [6] in the USA). A long straightedge (2m in Europe, 3m in the USA) is used to control *global* flatness (*i.e.* larger deformations, like bending), while a smaller ruler (0.2m in Europe, 0.3m in the USA) can be used to control *local* flatness (little gaps or bumps).

The Straightedge method is simple to understand and inexpensive, and thus still used for controlling surfaces with low-level flatness specifications. However, it presents important deficiencies including: the difficulty of test large areas of floors in reasonable times; the poor precision of the measurements; the inability to reproduce results. For these reasons, alternative approaches for floor profiling have emerged that make use of modern measuring technologies and are somewhat simpler to implement, such as: the F-Numbers method and Waviness Index method.

F-Numbers method [5, 6, 7]. The F-numbers method may be seen as a modern extension of the Straightedge method, making use of modern and

more precise measurement technology, such as optical levels, total stations, inclinometers or longitudinal differential floor profilometers [6, 7].

The F-Numbers measurement method is described in detail in ASTM E 1155-96 [7]. It consists in defining a grid of floor profile survey lines (separated by at least 4 ft) on the surface of each floor section, measuring point elevation at regular 1 ft (~ 0.3 m) intervals along each line, and finally calculating the F_F and F_L values that summarize the floor profile:

- \mathbf{F}_F is a statistically calculated number that takes into account the mean and standard deviations of sample measurements of 12 in (~ 0.3 m) incremental curvatures. F_F thus estimates the floor's flatness; and
- \mathbf{F}_L is a statistically calculated number that takes into account the mean and standard deviations of sample measurements of 120 in (~ 3 m) elevation differences. F_L thus estimates the floor's levelness.

While the F-Numbers method is a clear improvement over the Straight-edge method, its downside is that it is mathematically more complex, and the reported F-Numbers are unitless and are therefore difficult to comprehend. Additionally, the F-Numbers is that does not readily provide information on the location of defects on the floor. Last, but not least, it has been shown to react to floor undulations (*i.e.* defects) with period 1.5-4 ft (F_F) and 15-80 ft (F_L), which provides a fairly incomplete analysis of the surface waviness. This is particularly problematic when forklifts are to be operated on the floor (a very common case). Indeed, it has been theorised that surface undulations that can affect the operation of forklifts range between 50% and 100% of their wheelbase length [8, 9], which typically translates to the range from 2 ft to 10 ft.

Waviness Index (WI) method [10]. This method was conceived as a result of the lack of responsiveness of the F-Numbers method to floor undulations of periods between 2 ft and 10 ft [8, 9]. The WI method follows essentially the same measuring procedure as the F-Numbers method. Measurements are conducted at regular 1 ft intervals along floor survey lines, and deviations are calculated from the midpoints of imaginary chords defined by pairs of measured points along the survey line. In its standard form, the method considers chords of lengths $2k$ ft where $k \in \{1, 2, 3, 4, 5\}$, that is lengths of 2, 4, 6, 8 and 10 ft (60, 120, 180, 240 and 300 cm) [9]. Another advantage of the WI method is that its results express the deviation from flatness in inch (or centimetre), and are thus much simpler to comprehend than the F numbers.

The three methods above show an evolution over time that aimed to address the limitations of previous methods and make use of new measuring technologies. The Waviness Index method can be seen as the current state-of-the-art method, particularly for its consideration for a range of undulation periods, as opposed to just one or two [9]. Yet, the Waviness Index method still presents three main limitations:

1. Like all its predecessors, the WI method is still based on sparse measurements conducted along survey lines that are themselves sparsely spaced. As a result, the overall flatness assessment results may be inaccurate, with defective floors/slabs not being detected. The use of sparse measurements was motivated by (1) the lack of measuring device that could deliver both dense and accurate measurements across slabs in a timely manner, and (2) the significant human input required for measuring and later calculating the flatness characterisation values.
2. The WI method considers five different waviness periods in its analysis. Although these are homogeneously spread from 2 ft to 10 ft, one could argue that this presents an additional level of sparsity in the analysis that can further impact the reliability of the flatness characterisation. In fact, we will show later through experimental results that the WI method is actually quite imprecise in detecting undulations with short periods, in particular 2 ft.
3. The WI method, like the F-Numbers method, does not readily report the locations of the defects along the survey lines. For exactly, information is available about the elevation profile and undulations of different periods, but their relative impact on the overall floor flatness value cannot be easily identified.

1.2. Terrestrial Laser Scanning (TLS) for Surface flatness control

Terrestrial Laser Scanning (TLS) is a modern measurement technology that is revolutionizing dimensional surveying in the Architectural, Engineering, Construction and Facilities Management industry (AEC&FM). As highlighted in numerous previous research works (*e.g.* [11, 1, 12, 13]), TLS provides surveyors with the means to conduct accurate and extremely dense 3D measurements in relatively short times, which should in turn lead to more reliable dimensional control results. Focusing on flatness control, dense measurements over an entire surface should enable the assessment

of flatness more comprehensively and reliably. This would be a significant
110 advantage over the traditional methods discussed earlier that are based on
sparse measurements.

Many researchers have developed approaches to compute and display
the deviations of laser scanned points from reference surfaces for visual
inspection of surfaces [1, 12, 14, 15]. However, these works focused on
115 visualisation and did not consider the issue of detecting and characterizing
surface flatness defects.

Tang et al. [13, 16] then developed three algorithms to detect and char-
acterise flatness deviations in TLS data. Their main algorithm works in
three stages: (1) Apply Gaussian noise filtering to the point cloud; (2) Fit
120 a plane against the overall point cloud; and (3) Calculate the distance be-
tween each point and the overall plane. Two other variant algorithms are
also considered. Although analyzed with a certain level of detail, the meth-
ods presented by Tang et al. focus on detecting picks in the deviations, *i.e.*
undulation amplitudes, as opposed to characterising surface waviness. As
125 discussed earlier, waviness assessment is central to surface flatness charac-
terisation. Therefore, while the work of Tang et al. certainly contributes in
demonstrating the potential of TLS for conducting surface flatness assess-
ment, their proposed methods would provide insufficient results to draw full
conclusions on surface flatness.

130 Bosché and Guenet [17] digitally encoded the Straightedge and F-Numbers
methods so that they can be automatically applied to the TLS point clouds
of floors. A comparison of the results obtained by the encoded Straightedge
method with those obtained by manually applying the Straightedge method
on the slab also confirmed that TLS data appears to provide point clouds
135 that are sufficiently accurate and precise for detecting and characterising
subtle defects like small floor flatness undulations. The advantage of the
work of Bosché and Guenet is that it employs existing survey methods (ap-
plied digitally) so that practitioners can better assess the value of TLS for
such measurements. But, the limitations inherent to those methods remain,
140 that is:

1. They are designed to be conducted with only sparse measurements and
therefore provide incomplete analysis. Although Bosché and Guenet
show that this limitation can be addressed by increasing the number
of straightedge measurements or F-Numbers survey lines around the
145 floor.
2. They characterise surface waviness by considering only one or two

surface undulation periods (1.5-4 ft and/or 15-80 ft).

3. All existing methods characterise surface waviness by analysing waviness along lines, *i.e.* in 1D. While this may be justified in the case of floors with defined wheel-track traffic (narrow aisles), floors with random traffic should preferably be assessed in 2D.
4. The F-Numbers method enables the detection of flatness defects, but does not naturally report their *location* on the surface.

As we show later, applying the Waviness Index method to TLS point cloud data would partially address the second limitation, because that method considers a set of five undulation periods. However, the third and fourth limitations remain for all methods.

1.3. Contribution

We propose a new method for conducting surface flatness control using TLS data. The method aims to address all the limitations of existing methods identified above. The idea is to conduct a frequency analysis of the TLS points associated to a surface, using Wavelet Transforms, more particularly the Continuous Wavelet Transform.

As discussed earlier, all existing methods (Straightedge, F-Numbers, *etc*) are in some way based upon frequency analysis, but are significantly simplified due to the limits of the sensing technologies available at the time when they were designed, in particular the impossibility to conduct very dense accurate measurements. TLS has now changed this situation entirely, so that new ways of conducting flatness control can be devised that take advantage of the density and quality of measurements provided by TLS to deliver more precise results in terms of flatness defect detection, characterisation and localization.

The rest of this paper is organized as follows. Section 2 first reviews different frequency analysis methods leading to the selection of the Wavelet Transforms, and more particularly the Continuous Wavelet Transform. The proposed approach and implemented system are then presented in Sections 3. Results of the experiments conducted to test and validate the proposed approach are reported and discussed in Section 4. Conclusions are finally drawn and recommendations for future research suggested in Section 5.

2. Fourier and Wavelet Transforms

In the case of surface flatness control, one can assimilate the measured elevation profile along a survey line as a discrete 1D surface waviness ‘sig-

nal’. More generally, the elevation profile over the entire surface can be assimilated to a discrete 2D ‘signal’. In both cases (1D and 2D) frequency analysis techniques can be considered in order to detect the presence of undulations with certain frequencies (*i.e.* periods), and thereby detect construction defects.

2.1. Fourier Transform (FT)

It is well-known that any continuous signal can be re-written, or decomposed, as the sum of sinusoidal functions with varying amplitudes and frequencies, altogether known as the frequency spectrum. This process, when applied to continuous signals is known as the Fourier Transform (FT). In engineering practice, signals are not continuous but discrete, in which case the corresponding Discrete Fourier Transform is applied.

The FT gives information on frequency components over the entire length of the signal. Thus, while it permits to estimate in which “quantities” different frequencies exist, it is unable to provide the location along the signal where they are present. FT is thus suitable for stationary signals where frequency content does not change in time, but is not suitable for non-stationary signals where frequency content changes over time (in our case, over space). Since surface waviness is a non-stationary signal, applying the FT to elevation profiles could enable the detection of defects (*i.e.* undulations of certain periods and amplitudes) but would not enable their localization along the signal; the latter being critical information to correct the defects.

2.2. Short Time Fourier Transform (STFT)

The idea of the Short Time Fourier Transform (STFT) is to process non-stationary signals in segments, which are themselves assumed to be stationary. To isolate individual segments of the input signal – a process called *windowing* – the signal is multiplied by a square function that is incrementally translated along the signal; note that the STFT uses a window of fixed width. The FT is then computed for each windowed signal segment. The output of the STFT is a 3D diagram representing amplitude responses for different frequencies at different locations along the signal.

In our context, the multiplication of the original signal by a translated square function should a priori support the localization of the different frequencies. However, signal windowing using a fixed square function with fixed width has some significant downsides. First, the process results in some loss of accuracy in the frequency domain. Then, it prevents it to

220 achieve good *resolution* in time and frequency simultaneously. As discussed
in Section 1.1, surface flatness assessment requires a fairly wide range of
frequencies to be analysed – periods between 2 ft and 10 ft. With a 10 ft
window, the STFT would achieve the detection and localization of a sig-
225 nal with period 10 ft with the best accuracy possible. However, it would
be fairly poor for the localization of undulations of period of 2 ft – *i.e.* if
such a 2 ft period is detected, the user will only know that it is somewhere
within this 10 ft window. In contrast, a 2 ft wide window will enable the
detection and localization of undulations with period 2 ft with great accu-
230 racy, but would not support the detection of undulations with period 10 ft.
This illustrates the difficulty, in fact the impossibility, to simultaneously
achieve good precision in space/time and frequency; a problem known as
the *Heisenberg uncertainty* principle.

Nonetheless, this impossibility is not necessarily critical in practice. Indeed,
it has been observed that for many real-life problems, including that of
235 surface flatness control, the precision required for localizing low frequency
signals is generally lower than that required for high frequency signals. This
important observation has motivated the development of new methods, in
particular the Wavelet Transform.

2.3. Wavelet Transform (WT)

240 The Wavelet Transform (WT) is presented in detail in countless publica-
tions, including [18, 19]. While we provide a summary of it in the following,
we invite the reader to explore such publications for more detail.

The WT analyses a signal by convolving it with a function, called the
wavelet, at incremental locations along the signal and at incrementally in-
245 creased scales. The wavelet is designed/selected to detect a certain type
of pattern/frequency (see Figure 2). The incremental increase in scale can
be seen as a simultaneous increase in the ‘window’ of signal considered and
decrease of frequency examined. In other words, low frequencies are only
250 examined at large scales (*i.e.* with large windows) and high frequencies are
only examined at small scales (*i.e.* with narrow windows), thereby opti-
mally dealing with the Heisenberg uncertainty principle. This is commonly
illustrated with the diagrams reproduced in Figure 1,

The output of the WT when applied to a 1D signal is a 3D representation
of the response of the convolution of the signal with the wavelet for different
255 values *translation* τ and *scale* a . The scale a in WT bears some equivalence

with some characteristic frequency f ($a \sim 1/f$). This is discussed further later.

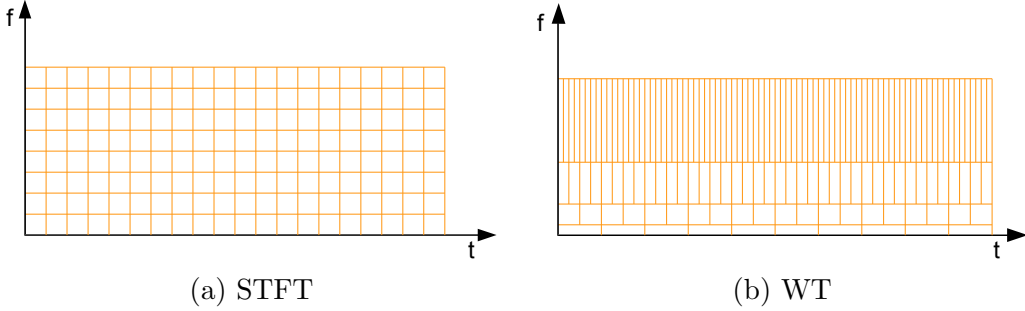


Figure 1: Comparison of the STFT and WT time-frequency resolutions. All cells in both graphs have the same surface areas, illustrating the Heisenberg principle.

2.3.1. Mother Wavelets

The wavelets used at the different scales are all obtained by dilating a *mother wavelet*. To ensure a strong response of the convolution the mother wavelet should present a shape similar to that searched in the signal. As a result, many mother wavelet functions have been proposed for different applications. Some commonly used ones include: the *Mexican Hat*, the *Morlet*, the *Daubechies* or the *Bior* functions (see Figure 2).

For surface flatness control, the type of ‘defect’ to be examined typically has a shape of a ‘*smooth bump*’ or, from a signal viewpoint, one period of a sinusoidal signal. In this context, the *Mexican Hat* wavelet (Figure 2a) appears quite well suited.

2.3.2. Continuous, Stationary and Discrete Wavelet Transforms

In parallel to the selection of mother wavelets, various WT methods can be distinguished, in particular: the *Continuous Wavelet Transform (CWT)*, *Stationary Wavelet Transform (SWT)*, and *Discrete Wavelet Transform (DWT)*.

As illustrated in Figure 3, the CWT aims to analyse the input signal with full resolutions in both translation and scale. On the other end, the DWT applies a two-dimensional dyadic decomposition that results in ‘skipping’ levels of precision in translation and scale. In between lies SWT that ‘skips’ levels of precision in scale using the same dyadic decomposition approach as the DWT, but retains the same precision in localization (translation) as the CWT.

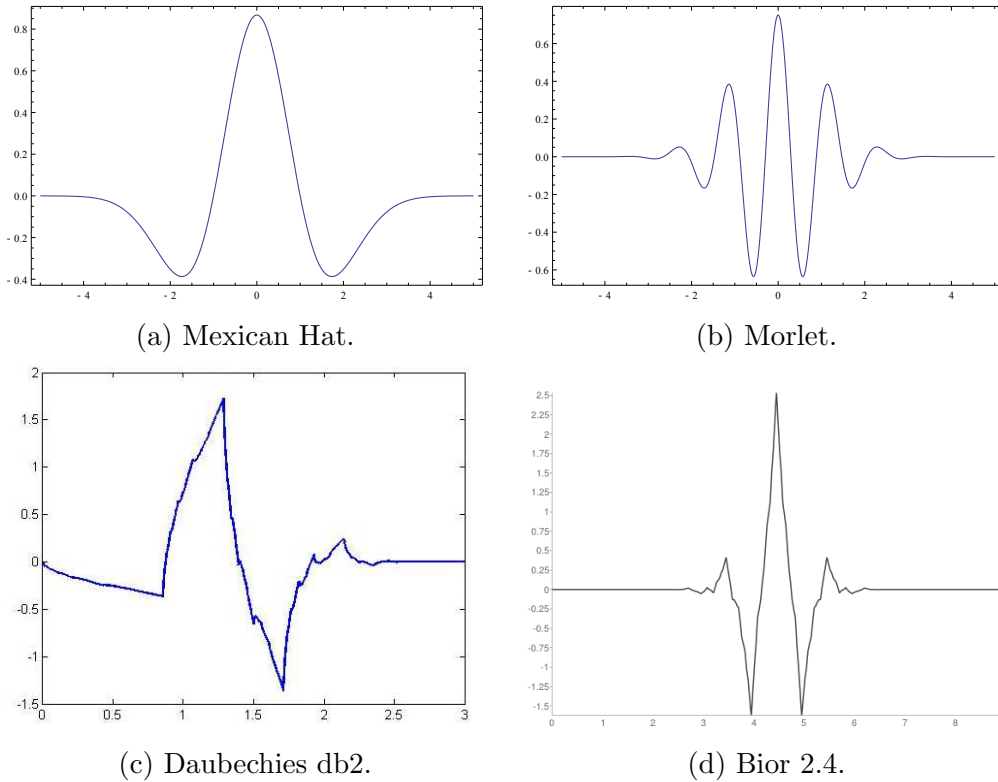


Figure 2: Four examples of mother wavelet functions: the Mexican Hat and Morlet wavelets are used with the CWT, and the Biorthogonal 2.4 (bior 2.4) and Daubechies 2 (db2) wavelets are used with the SWT/DWT.

285 The difference between these three WT approaches actually goes beyond the resolutions they consider in localization and frequency, even requiring different types of wavelets. The reason is that they have actually been developed for totally different purposes. The CWT is aimed at detecting a (wavelet) pattern/frequency accurately in both location (translation) and scale. In contrast, the DWT aims to capture as much as possible of the information contained in a signal at the least cost possible; it is mainly used for signal compression (*e.g.* the JPEG2000 format in image compression). The SWT provides a trade-off that has a practical value in some engineering

290 problems where the detection and localization of a pattern in a signal needs to be known with sufficient accuracy, but the scale of the searched pattern (frequency) may a priori not be known with great precision. Focusing on the context of floor flatness assessment, it can be concluded that the CWT appears to be the most appropriate approach — although the SWT may

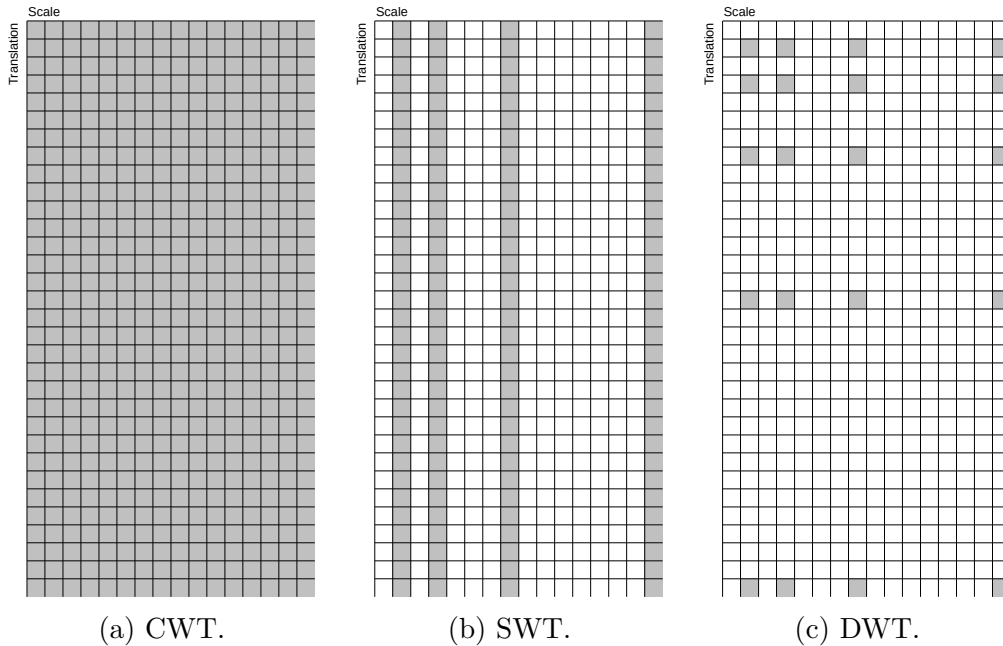


Figure 3: Comparison of the CWT, SWT and DWT in terms of the resolutions in scale and translation they provide. Each box corresponds to one increment unit along the axis; the grayed boxes are those computed by the method.

295 still apply. In contrast, the DWT does not suit this kind of problem at all.

Note that, of the wavelets shown in Figure 2, the Mexican Hat or Morlet wavelets are used for the CWT, while the Daubechies or Bior wavelets are used for DWT and SWT.

2.3.3. The relation between the scale a and the characteristic frequency f

300 As pointed earlier, there is a relation between the scale a at which a wavelet is applied and a *characteristic frequency* f that it reacts to. This relation depends on the mother wavelet and is given by the formula [19]:

$$f = \frac{f_c}{\delta_p a} \quad (1)$$

where f_c is the *center frequency* of the mother wavelet (*i.e.* the main frequency component of the FT of the mother wavelet) and δ_p is the point sampling period (along the signal). A strong response of the convolution of the wavelet at scale a thus indicates the presence of an undulation with frequency f .

The *characteristic period* \mathbb{T} of the signal is easily derived from Equation 1 as:

$$\mathbb{T} = \frac{1}{f} = \frac{\delta_p a}{f_c} \quad (2)$$

310 Table 1 provides the center frequency and the resulting characteristic frequency and period for different wavelets, for $a=1$ and $\delta_p = 1 \text{ cm}$.

Wavelet	f_c	a	f (cm^{-1})	\mathbb{T} (cm)
Mexican Hat	0.252	1	0.252	4.0
bior2.4	0.889	1	0.889	1.1
db2	0.667	1	0.667	1.5

Table 1: Center frequency f_c for some commonly employed wavelets, and the corresponding characteristic frequency f and period \mathbb{T} for $a=1$ and $\delta_p = 1 \text{ cm}$.

2.3.4. 1D and 2D Analysis

The WT, like the FT and STFT, can be applied to multi-dimensional signals, not just one-dimensional ones. In the context of floor flatness assessment, this means that WT could be applied not just to elevation profile data along a survey line (1D signal), but also to 2D elevation profile data for an entire surface at once.

320 The process followed in the 2D WT consists in convolving the wavelet with the signal along two orthogonal directions. Those results then can be combined to establish frequency responses in intermediary directions [20].

2.4. Conclusion

The discussion above suggests the potential of the CWT for the detection and localization of flatness defects. In this paper, we present results of the application of the 1D CWT to elevation profiles obtained along survey lines virtually generated with the TLS point cloud data of construction slabs. Applying the CWT in 1D is particularly valuable to compare its results with those obtained with existing methods, in particular the Waviness Index method. If the results are positive, then, as suggested in Section 2.3.4, future work should certainly pursue applying the CWT approach directly to 2D TLS point clouds of floors.

3. Surface Flatness Control using the Wavelet Transform

We have implemented a 1D CWT-based algorithm to process TLS point cloud data of planar surfaces with the aim to assess its suitability for flatness

control in construction. The algorithm has actually been implemented on
335 top of an existing *Scan-vs-BIM* platform [17] – *i.e.* a system enabling the
segmentation of as-built (TLS) point clouds by aligning them with the as-
designed 3D (BIM) model of the facility and segment the point cloud based
on spatial proximity and local normal similarity. Within the context of this
paper, the system particularly enables the segmentation of the subset of
340 points corresponding to a given floor. The same platform was used in [17]
where we reported previous results on the application of the Straightedge
and F-Numbers method to TLS data.

The 1D CWT algorithm applies the CWT to surface elevation profiles
obtained along survey lines virtually surveyed ‘in’ the TLS data of the
345 surface. In order to assess the performance of the method, we have also
uniquely developed another algorithm that automatically applies the Wavi-
ness Index (WI) method to the same survey lines. This enables the com-
parison of their respective results, and thereby the validation of the use of
the CWT for surface flatness control.

350 Both algorithms apply the same automated pre-processing to the data,
described in Section 3.1 below. The implementation of the WI method is
detailed in Section 3.2 and that of the 1D CWT method in Section 3.3.

3.1. Pre-processing

3.1.1. Point cloud data organization

355 The procedures described below for the WI (Section 3.2) and the CWT
(Section 3.3) include different stages requiring nearest-neighbour searches
within the floor’s TLS point cloud. Because a laser scan of a floor surface can
easily contain millions of points, an exhaustive search would be extremely
inefficient. As a result, a 2D square array structure is implemented where
360 each cloud point is associated to one of the array cells. Nearest-neighbors
are then searched only among the points contained in the cells neighboring
the given input location. As illustrated in Figure 4, the orientation and
extent of the array are determined using the two main directions of the
floor and a pre-defined array cell size, d_{array} (we use $d_{array} = 50mm$). For
365 more detail, we refer the reader to [17], where the same structure was used
in the implementations of the Straightedge and F-Numbers methods.

3.1.2. Noise filtering

All surface flatness assessment methods are based on the measurement
of the deviation of points from the reference surface. To reduce the effect of
370 laser scanning measurement imprecision on the estimation of each point’s

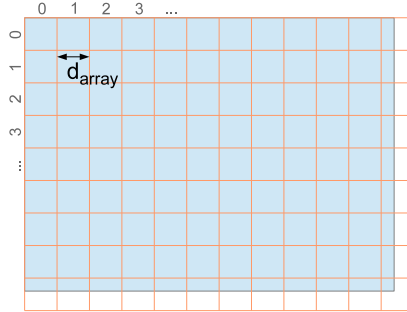


Figure 4: Illustration of the 2D square array structure used to accelerate nearest-neighbor searches. The blue rectangle is the floor’s top face, and the array is shown in orange (reproduced from [17]).

deviation, a mean filter is applied across the point cloud, where each point’s deviation is re-calculated as the average of the deviations of its neighbors within a neighborhood ρ . We use $\rho = 25 \text{ mm}$.

3.2. Waviness Index Method

375 ASTM-E1486 [10] specifies a standard procedure for the application of the WI method, that is summarised here.

First, survey lines are defined parallel to the principal axes of the surface, spaced by no more than $\delta_\ell = 30 \text{ ft}$ — in the experiment reported later we use $\delta_\ell = 1 \text{ ft}$ ($\sim 0.3 \text{ m}$). In contrast with the F-Numbers method, 380 the Waviness Index method does not prohibit survey lines from crossing control and construction joints. However, survey lines should similarly not extend too close to other building elements like columns and walls. In our implementation, we assume that the boundary of the test surface is known, and we prevent survey lines from extending closer to the surface boundary 385 than d_{boundary} . In the experiments reported below, we use $d_{\text{boundary}} = 30 \text{ cm}$.

Then, survey points, *i.e.* elevations, are measured at intervals of $\delta_p = 1 \text{ ft}$ along each survey line, using the approach described in Section 3.1.2.

Each survey line should contain at least 15 measurements, and the minimum total number of survey points in a test section should be $A/16$, where 390 A is the section surface area in ft^2 . If these requirements are fulfilled (which is easily checked algorithmically), then various Waviness Index results can be calculated using the formulas provided in ASTM-E1486 [10]. First, it is possible to calculate the WI response for each level k for each the survey

line ℓ , using the equation:

$$LAD_{\ell,k} = \sqrt{\frac{\sum_{i=1}^{imax_{\ell,k}} (LAD_{\ell,k,i})^2}{imax_{\ell,k}}} \quad (3)$$

395 where $LAD_{\ell,k,i}$ is the WI response at the level k at the i^{th} sampled location along the line ℓ ; $imax_{\ell,k}$ is the number of incremental locations where the WI response is calculated along the line ℓ at level k ; $k \in \{1, 2, 3, 4, 5\}$

Then, $LAD_{\ell,k}$ values obtained for the five k level (*i.e.* five undulation periods) can be aggregated to calculate the overall WI response for each
400 line, using the equation:

$$WI_{\ell} = WI_{\ell,2-10} = \sqrt{\frac{\sum_{k=1}^{kmax} (imax_{\ell,k} (LAD_{\ell,k})^2)}{n_{\ell}}} \quad (4)$$

where $kmax = 5$ and $n_{\ell} = \sum_{k=1}^{kmax} imax_{\ell,k}$.

Finally, the WI_{ℓ} values obtained for all lines can be aggregated to calculate an overall WI response for the entire floor, using the equation:

$$WI = WI_{2-10} = \sqrt{\frac{\sum_{\ell=1}^{\ellmax} (n_{\ell} (WI_{\ell})^2)}{\sum_{\ell=1}^{\ellmax} n_{\ell}}} \quad (5)$$

where ℓmax is the number of measured survey lines.

405 Note that if fewer than 15 measurements are available for a line, it is still possible to apply the formulas above. But, in such case, $kmax$ will have to be set lower than 5, and consequently WI_{ℓ} (and WI) will have to be calculated as $WI_{\ell,2-8}$ or $WI_{\ell,2-6}$.

3.3. 1D CWT Method

410 The proposed algorithm for conducting a 1D CWT-based flatness control applies the CWT to elevation profile measurements acquired along survey lines. The algorithm uses the same survey line generation and survey point measurement methods as the Waviness Index method, which enables a fair

comparison of the approaches. However, instead of $\delta_p = 1 \text{ ft}$ (as specified
415 for the Waviness Index method), we make use of the density of measure-
ments provided by the laser scanner and instead measure survey points with
intervals $\delta_p = 1 \text{ cm}$.

The mother wavelet should be selected so that it enables a good detection
of the searched pattern in the signal. As discussed in Section 2.3.1, we have
420 selected the *Mexican Hat (MH)* as a suitable wavelet for applying the CWT
to assess waviness.

The scale at which the wavelet is applied enables the detection of pat-
terns of similar scale. In our context, we are looking for signal undulations
(*i.e.* defects) of different periods, that is at different scales. Given the se-
425 lected wavelets, Table 2 summarizes at which scales/levels the CWT and
WI methods should provide approximately comparable results, *i.e.* respond
to the same characteristic period. This is an interesting table that high-
lights an important advantage of the CWT method that is the resolution
(*i.e.* precision) that it provides in the frequency domain. This is in addition
430 to its high resolution in the spatial domain and its efficient visual represen-
tation of the results enabling fast localization of defects (as demonstrated
later).

Note that our systems employs the *cutlib* C++ code library [21] for the
application of the CWT.

435 4. Experimental Results of Preliminary Investigation

4.1. Datasets

We have conducted preliminary experiments using two existing concrete
slabs of university laboratories. The slabs are the same as those used in [17].
The *Drainage Lab (DL)* slab is $4.8\text{m} \times 8.1\text{m}$ and the *Acoustic Lab (AC)* slab
440 is $6.4\text{m} \times 6.7\text{m}$. The two slabs have been laser scanned using the Faro Focus
3D scanner [22] with standard resolution, and medium-high data acquisition
quality. The AL slab required two scans that were merged using standard
registration methods. After segmenting the two scans, The DL slab's cloud
contains 0.50 million points, while the AL slab's point cloud contains 1.3
445 million points. Figure 5 shows the two slabs and the point clouds associated
to them.

4.2. Results

Figure 6 shows the survey lines automatically generated and surveyed for
the DL and AL floors. The figure also shows the elevation profiles measured

T	CWT	WI
	a	k
4	1	
⋮		
8	2	
⋮		
12	3	
⋮	⋮	
60	15	1
⋮	⋮	
120	30	2
⋮	⋮	
180	45	3
⋮	⋮	
240	60	4
⋮	⋮	
300	75	5

Table 2: Mapping of the CWT scales (using the Mexican Hat wavelet) against the Waviness Index k levels, assuming a point spacing of 1 cm for CWT and 30 cm (approx. 1 ft) for the Waviness Index. T is the characteristic period of the corresponding detectable surface undulations. The colouring highlights the a and k pairs at which the two methods should provide comparable results. The sign $\dot{}$ indicates that other values are available in-between; this highlights the significantly higher resolution (precision) of the CWT method in the frequency domain.

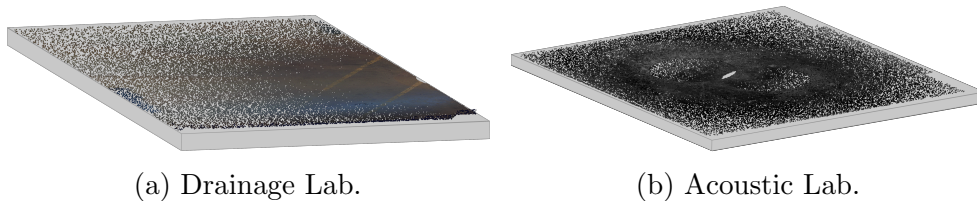


Figure 5: The DL and AL slabs with their associated point clouds.

450 from six of the lines (those further analysed below).

Figures 7 and 8 show the results obtained with the CWT and WI methods for three survey lines of the DL slab and three survey lines of the AL slab respectively (the locations of these lines on the slabs are indicated in Figure 6). The selected survey lines have different lengths as well as dif-

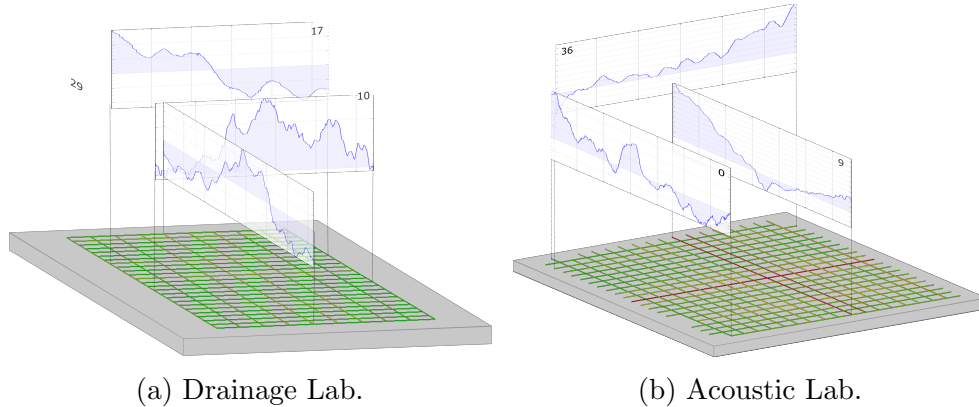


Figure 6: The survey lines generated for the DL and AL slabs. The six survey lines further analysed in Figure 7 (DL) and 8 (AL) are identified.

455 ferent profiles (Figures 7a and 8a) presenting potential defects with various undulation periods. The WI results in Figure 7c confirm that the first reported survey line of the DL slab presents minor deviations with respect to the investigated half-periods, *i.e.* 60 cm, to 180 cm. In contrast, the WI results for the second reported survey line of the DL slab suggest the presence
 460 of more significant undulations with these periods; and this can indeed be visually confirmed in the profile data. The second reported survey line of the AL slab appears to have significant undulations with periods of 240 cm and 300 cm; again, this can be confirmed in the profile data (mid-length). These results illustrate the value of the WI method for floor flatness control

465 More importantly here is the comparison of the CWT results with those obtained with the WI method. The CWT results are presented in 2D colormaps that are commonly called *scalograms*. Some parts of the CWT scalograms shown in Figures 7b and Figures 8b are purposely shaded because the corresponding locations along the survey lines are where, at the given scale, the most important parts of the wavelet would fall outside the profile; the corresponding results are thus not meaningful and should be
 470 discarded.

Focusing on the meaningful part of the scalograms, it can first be noted that the CWT results can be both negative or positive. A negative value
 475 indicates a negative correlation when convolving the signal with the wavelet (*i.e.* concave undulation), and a positive value indicates a positive correlation (*i.e.* convex undulation). Then, the vertical alignments of the profiles

(7a) with the scalograms (7b) indicate that the CWT seems to successfully detect surface undulations with the correct periods, and with higher strengths when the undulations present higher amplitudes. For example, the third reported profile line of the DL slab clearly shows an undulation of period 300-400 cm that is well detected and located by the CWT method. The 50 cm undulation on the right side within that large undulation is also clearly detected. For the third reported line of the AL slab, the CWT nicely detects and locates the numerous undulations of short period (~ 50 cm) along the line, but also correctly does not detect any meaningful undulation with period longer than 100 cm.

An overall and more scientific comparison between the CWT and WI results can be conducted by looking at the correlation between the responses of the two methods for similar periods for the same elevation profiles. To perform the comparison, we propose to calculate CWT responses $CWT_{\ell,a}$ corresponding to the WI $LAD_{\ell,k}$ values using the same root mean square (formula (Equation 3)), that is:

$$CWT_{\ell,a} = \sqrt{\frac{\sum_{i=1}^{imax_{\ell,a}} (CWT_{\ell,a,i})^2}{imax_{\ell,a}}} \quad (6)$$

where $CWT_{\ell,a,i}$ is the CWT response at scale a at the i^{th} sampled location along the line ℓ ; $imax_{\ell,a}$ is the number of sampled locations where the CWT response is calculated along the line ℓ at scale a .

We also calculate the CWT response for each line ℓ , CWT_{ℓ} , using the same formula as the one used to calculate WI_{ℓ} ((Equation 4), that is:

$$CWT_{\ell} = \sqrt{\frac{\sum_{a=1}^{amax} imax_{\ell,a} (CWT_{\ell,a})^2}{\sum_{a=1}^{amax} imax_{\ell,a}}} \quad (7)$$

where $amax$ is the number of scales considered. In the context of the comparison conducted here, this is the set of five scales $a \in \{15, 30, 45, 60, 55\}$ that give the same undulation characteristic periods as those considered by the WI method with $k \in \{1, 2, 3, 4, 5\}$. These characteristic period are $T(cm) \in \{60, 120, 180, 240, 300cm\}$ (see Table 2).

Figure 9 reports the correlation results. Figure 9a shows a scatter plot of the 295 pairs of WI $LAD_{\ell,k}$ and $CWT_{\ell,a}$ values obtained (for 75 survey

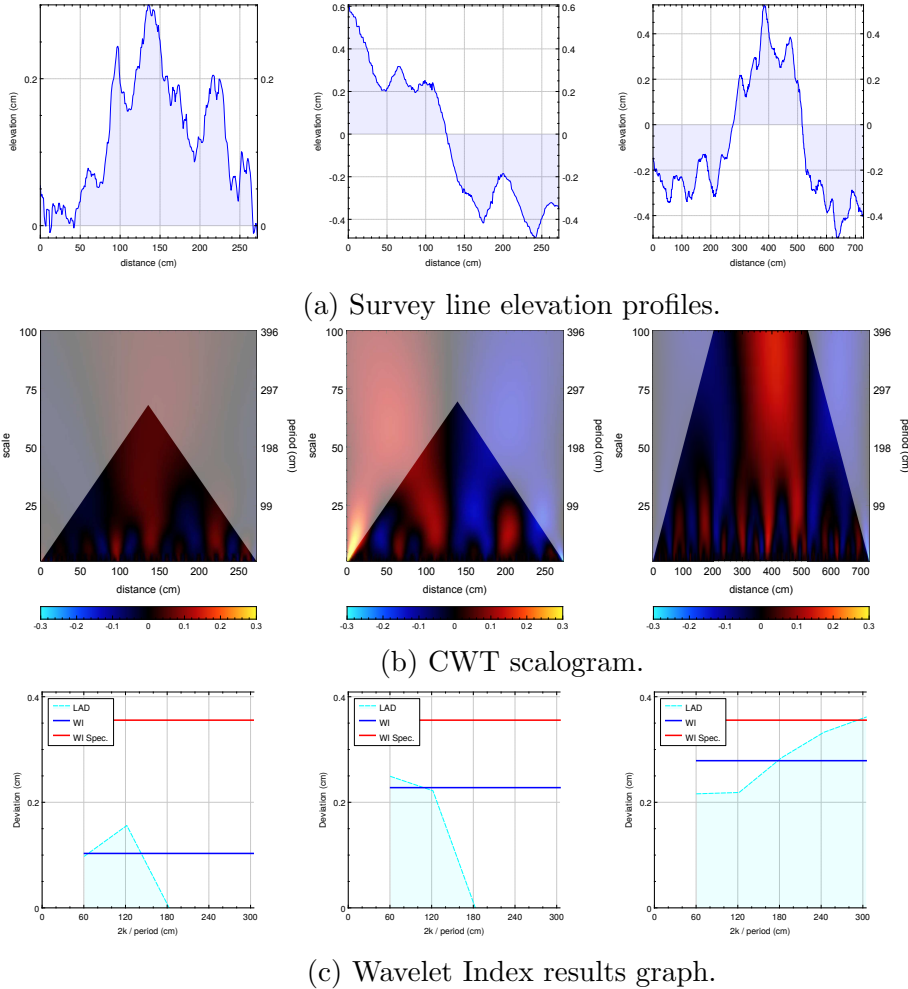


Figure 7: CWT and WI results for the analysis of three different survey lines obtained for the Drainage Lab (DL) slab.

lines, and the five k values and corresponding a values). Figure 9b then shows a scatter plot of the pairs of WI_ℓ and CWT_ℓ values obtained for all 75 lines.

The results in Figure 9a show a certain level of correlation between the WI and CWT results. In fact, the correlation R^2 value is only 0.67. The results in Figure 9b indicate an even stronger correlation when combining all five undulation periods. The correlation R^2 value is 0.84.

Altogether, these results show a good positive correlation between the WI and CWT responses, thereby confirming the value of the proposed ap-

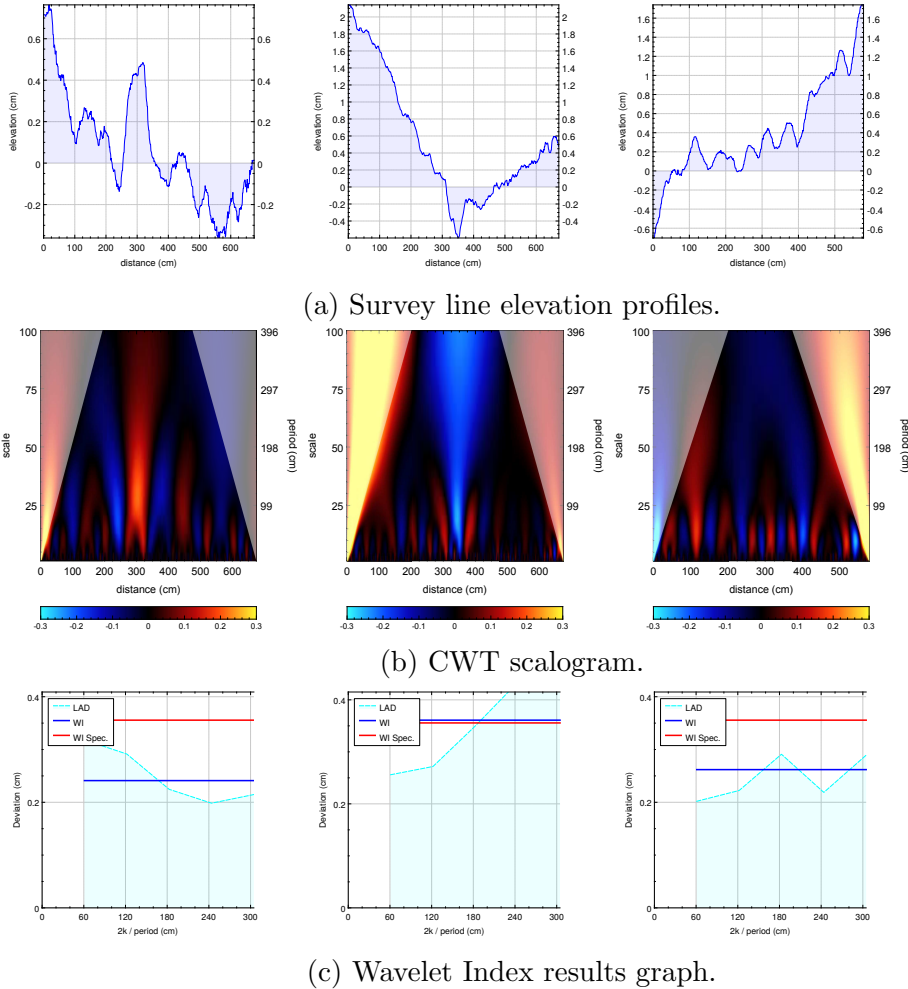
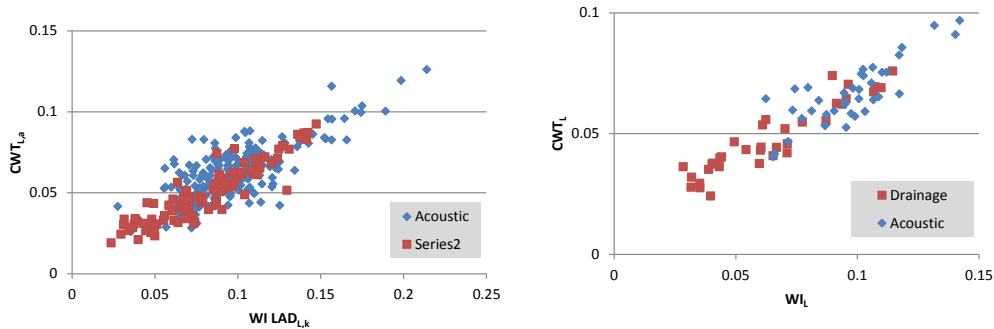


Figure 8: CWT and WI results for the analysis of three different survey lines obtained for the Acoustic Lab (AL) slab.

515 proach. Yet, it is interesting to note the apparent lower level of correlation
at the level of the undulation periods. A more detailed analysis of the re-
sults offers a likely explanation for this. It is observed that, when looking at
the correlation for the various undulation periods independently from one
another, the correlation is poorer for shorter undulation periods, especially
520 $T=60$ cm ($k = 1$), for which the $R^2 = 0.60$. Looking at the measurement
profiles considered by both approaches, it is observed that the measurement
sampling of the WI method ($\delta_p=30$ cm) can easily lead to inaccurate and
even failed detections of undulations of period 60 cm. Figure 10 shows



(a) Correlation between $CWT_{\ell,a}$ and $WI LAD_{\ell,k}$ responses for each of the five characteristic periods (60, 120, 180, 240 and 300 cm) and for each line.

(b) Correlation between CWT_{ℓ} and WI_{ℓ} responses for each line.

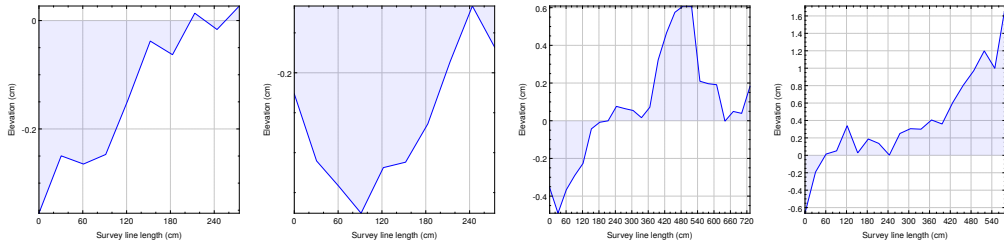
Figure 9: Assessment of the correlation between the CWT and WI responses using the data from the DL and AL slabs.

an example of elevation profile for four survey lines as measured using the
 525 WI method and the CWT method ($\delta_p=1$ cm). The analysis of the profiles clearly shows that while both methods capture with similar accuracy undulations with longer periods, the WI method leads to weaker detections of undulations with period 60 cm.

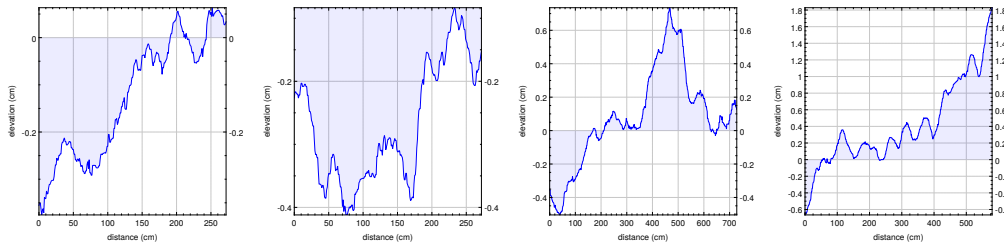
This highlights that the measurement sampling of 30 cm employed by the
 530 WI method is too sparse to enable an accurate detection of undulations with period 60 cm. In contrast, the dense measurement employed in the proposed approach leads to more accurate detections of undulations with periods of 60 cm, and shorter. This most likely explains the weaker correlation observed in Figure 9a.

535 5. Conclusion and Future Work

Terrestrial Laser Scanning (TLS) constitutes a significant evolution, if
 not a revolution, to construction dimensional surveying. Its capacity to provide dense and accurate point clouds of its surrounding environment very fast leads to the possibility to rethink how dimensional surveying (*e.g.* for
 540 construction control) should be conducted. More specifically, where conventional dimensional surveying is based on (sparse) point measurements, the density of points provided by TLS offers the opportunity to refocus dimensional surveying on surface measurements.



(a) Survey line profiles measured in the Waviness Index method.



(b) Survey line profiles measured in the CWT-based method.

Figure 10: 1D elevation profiles as measured in the WI method (a), and the proposed CWT-based method (b).

An area where the potential value of the dense measurement provided by
 545 TLS can be easily understood is that of surface flatness. While conventional, state-of-the-art methods for surface flatness assessment are based on sparse point measurements along themselves sparse survey lines, a new approach has been proposed that aims to take advantage of TLS and the density of points it acquires. Further, the novel approach applies the 1D Continuous
 550 Wavelet Transform (CWT) to the dense point measurements along densely packed survey lines, with the following several significant advantages over current practice:

- The process is fully automated, with manual intervention only required for conducting the scanning (a fairly simple process).
- 555 • The data processing being fully automated, the density of survey lines can be increased significantly compared to current manual methods, thereby addressing the issue of the sparsity of survey lines faced by those methods.
- 560 • The CWT analysis is a frequency-based analysis, providing results with high resolution in the frequency domain. In contrast, the state-of-the-art Waviness Index method only considers five frequencies. In fact, we have also shown what seems to be the poor precision of the

Waviness Index method for detecting undulations of period 60 cm (and shorter), which constitutes an valuable additional contribution.

- 565 • The CWT analysis not only offers a high resolution in the frequency domain, but also offers a similarly high resolution in the spatial domain, enabling the precise localization of frequency detections along the survey lines. Taking spatial and frequency resolution into account, the proposed method has a resolution 450 (30×15) times higher than that of the Waviness Index method.
- 570 • The scalograms outputted by the CWT constitute a very effective way of visually communicating results, enabling easy identification of the amplitude and frequency of detected undulations, and differentiating between concave or convex undulations.

575 Preliminary experimental results using two concrete slabs have demonstrated these advantages.

While the proposed approach appears extremely promising, further work remains to be conducted to confirm its strength (superiority). First of all, additional experiments clearly need to be conducted with many more, also
580 larger, concrete floors with varying types of finishing. Then, a mapping between CWT response and various types of standard flatness levels also needs to be established. Finally, it is acknowledged that the results reported here are still based on a 1D analysis (along survey lines). Yet, as discussed earlier, it is theoretically possible to remove the need to generate survey
585 lines and instead directly apply the CWT to complete 2D elevation profiles.

Acknowledgement

The authors would like to acknowledge the Erasmus Programme and the Région des Pays de La Loire (France) for their support towards Baptiste Biotteau's research visit to Heriot-Watt University.

590 References

- [1] B. Akinci, F. Boukamp, C. Gordon, D. Huber, C. Lyons, K. Park, A formalism for utilization of sensor systems and integrated project models for active construction quality control, *Automation in Construction* 15 (2006) 124–138.
- [2] British Standards Institution (BSI), BS 8204 – Screeds, bases and in situ flooring, 2009.
- 595 [3] British Standards Institution (BSI), BS EN 13670:2009 – Execution of concrete structures, 2009.

- 600 [4] CONSTRUCT, The Concrete Structures Group, National Structural Concrete Specification for Building Construction, 4th ed., CONSTRUCT, The Concrete Structures Group, 2010.
- [5] American Concrete Institute (ACI), ACI 302.1R-96 – Guide for concrete floor and slab construction, 1997.
- [6] American Concrete Institute (ACI), ACI 117-06 – Specifications for tolerances for concrete construction and materials and commentary, 2006.
- 605 [7] ASTM International, ASTM E 1155-96 – Standard test method for determining F_F floor flatness and F_L floor levelness numbers, 2008.
- [8] R. E. Loov, Is the F-number system valid for your floor?, Concrete International 12 (1990) 68–76.
- [9] C. N. Ytterberg, Flatness Tolerances For Random-Traffic Floors, Technical Report, The Aberdeen Group, 1996.
- 610 [10] ASTM International, ASTM E 1486 – Standard test method for determining floor tolerance using Waviness, wheel path, and levelness criteria, 2010.
- [11] G. S. Cheok, W. C. Stone, R. R. Lipman, C. Witzgall, LADARs for construction assessment and update, Automation in Construction 9 (2000) 463–477.
- 615 [12] F. Bosché, C. T. Haas, B. Akinci, Automated recognition of 3D CAD objects in site laser scans for project 3D status visualization and performance control, ASCE Journal of Computing in Civil Engineering, Special Issue on 3D Visualization 23 (2009) 311–318.
- [13] P. Tang, B. Akinci, D. Huber, Characterization of laser scanners and algorithms for detecting flatness defects on concrete surfaces, ASCE Journal of Computing in Civil Engineering 25 (2011) 31–42.
- 620 [14] P. Fuchs, G. Washer, S. Chase, M. Moore, Applications of laser-based instrumentation for highway bridges., ASCE Journal of Bridge Engineering 9 (2004) 541–549.
- [15] T. Schafer, T. Weber, Deformation measurement using terrestrial laser scanning at the hydropower station of gabcikovo, in: INGEO 2004 and FIG Regional Central and Eastern European Conference on Engineering Surveying, FIG, Copenhagen, Denmark, 2004.
- 625 [16] P. Tang, B. Akinci, D. Huber, Characterization of three algorithms for detecting surface flatness defects from dense point clouds, in: IS&T/SPIE Conference on Electronic Imaging, Science and Technology, volume 7239, SPIE, 2009.
- 630 [17] F. Bosché, E. Guenet, Automating surface flatness control using terrestrial laser scanning and building information models, Automation in Construction 44 (2014) 212–226.
- [18] R. Polikar, The wavelet tutorial. the engineer’s ultimate guide to wavelet analysis, 2006.
- 635 [19] P. S. Addison, The Illustrated Wavelet Transform Handbook: Introductory Theory and Applications in Science, Engineering, Medicine and Finance, 1st edition ed., CRC Press, 2002.
- [20] P. Subirats, J. Dumoulin, V. Legeay, D. Barba, Automation of pavement surface crack detection using the continuous wavelet, in: ICIP, 2006, pp. 3037–3040.
- 640 [21] S. Karpenko, Cwt lib, continuous wavelet transform library, 2013. URL: <http://sourceforge.net/projects/cwtlib/>, last visited 5 December 2014.
- [22] FARO, FARO Focus3D – Features, benefits & technical specifications, 2013.